

FOCUS ISSUE: SEMICONDUCTOR GAMMA CAMERA—REVIEW ARTICLE

Clinical Performance of the Discovery NM530c in Japanese Patients

Satoshi Hida, MD

Received: April 1, 2016/Revised manuscript received: May 9, 2016/Accepted: May 18, 2016

© The Japanese Society of Nuclear Cardiology 2016

Abstract

The Discovery NM530 is a new generation of SPECT cameras equipped with semiconductor cadmium-zinc-telluride (CZT) detector technology. It provides a shorter scan time and reduces the patient's radiation exposure without loss of image quality compared with the conventional Anger camera. Combined supine and prone imaging with the Discovery NM530c is useful for reducing the false-positive rate in the infero-posterior or infero-lateral segment associated with supine imaging. As studied by multicenter registry, 74% sensitivity, 85% specificity, and 81% accuracy for left anterior descending coronary artery stenosis, 76% sensitivity, 89% specificity, and 85% accuracy for left circumflex coronary artery stenosis, and 72% sensitivity, 86% specificity, and 82% accuracy for right coronary artery stenosis were observed in detecting an angiographic diameter narrowing of $\geq 75\%$ on visual estimation. Using a low-dose technetium-99m (185/370 MBq) 1-day protocol with an effective dose of ≤ 5 mSv, CZT SPECT demonstrated an acceptable diagnostic yield in detecting a significant coronary stenosis as assessed by fractional flow reserve (FFR). As for limiting to 92 coronary lesions in which FFR was measured, stress SPECT showed 77% sensitivity, 91% specificity, and 84% accuracy, whereas the diagnostic value decreased to 52% sensitivity, 68% specificity, and 58% accuracy based only on visual estimation of $\geq 75\%$ diameter narrowing. In addition, the quantification of myocardial perfusion reserve derived by dynamic SPECT imaging using the Discovery NM530c may help identify balanced ischemia in patients with left main or 3-vessel disease.

Keywords: Cadmium-zinc-telluride, Coronary artery disease, Diagnostic performance, Image quality, Myocardial perfusion imaging, SPECT

Ann Nucl Cardiol 2016 ; 2 (1) : 125-130

See page 122

Myocardial perfusion imaging (MPI) with single-photon emission computed tomography (SPECT) is widely used not only for the diagnosis of coronary artery disease (CAD) but also for evaluating disease severity in clinical practice. Although interest in radiation exposure from medical imaging is increasing throughout the world, nuclear cardiologists are expected to reduce a patient's radiation exposure from MPI SPECT (1,2).

The new generation of SPECT cameras equipped with semiconductor cadmium-zinc-telluride (CZT) detector technology is reported to provide superior image quality, reduced acquisition times, and lower radiotracer doses than the

conventional Anger camera (3-6).

Two dedicated CZT cameras, the Discovery NM530c (GE Healthcare, Haifa, Israel) and the D-SPECT (Spectrum Dynamics, Caesarea, Israel) are currently available for cardiac SPECT in clinical practice in Japan. In this review, I will focus on reports from Japan regarding the clinical performance of the Discovery NM530c.

Characteristics of the Discovery NM530c

The characteristics of the Discovery NM530c are described briefly as follows. The Discovery NM530c is equipped with a multiple-pinhole collimator and 19 stationary CZT detectors that simultaneously focus on the heart to maximize the efficiency of SPECT. The stationary array simultaneously

doi : 10.17996/ANC.02.01.125

Satoshi Hida

Department of Cardiology, Tokyo Medical University, 6-7-1

Nishishinjuku, Shinjuku-ku, Tokyo, Japan 160-0023

E-mail:hida-bin@tokyo-med.ac.jp

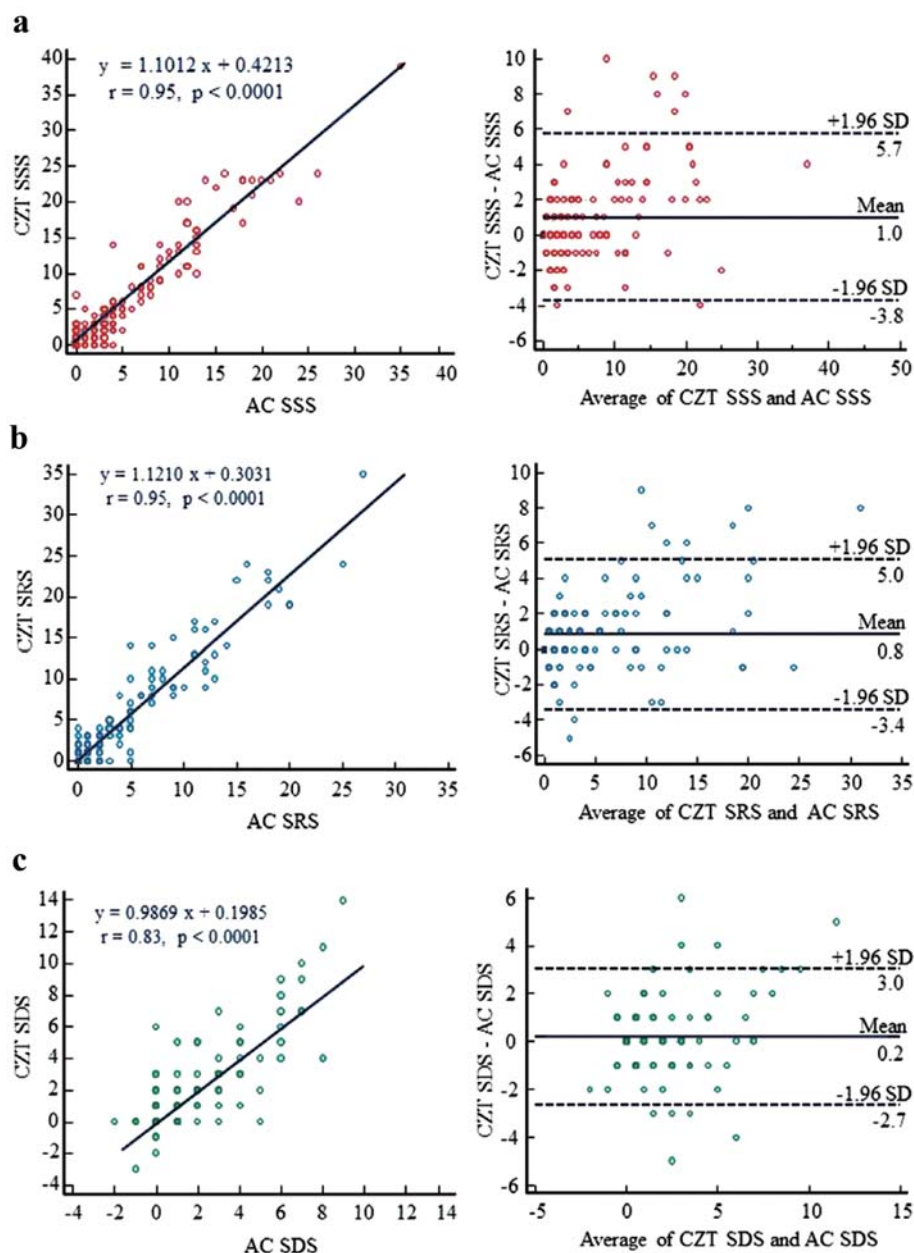


Fig. 1 Comparison of the summed scores between the CZT and the standard Anger cameras. (left) Linear regression analysis and (right) Bland-Altman plots for (a) summed stress score (SSS), (b) summed rest score (SRS), and (c) summed difference score (SDS) between the cadmium-zinc-telluride (CZT) camera and the standard Anger camera (AC). Reproduced with permission from Tanaka et al (6).

acquires all the views necessary for tomographic reconstruction, saving the time required by conventional cameras for acquisitions while rotating around the subjects (6). The energy resolution and spatial resolution are improved by a factor of 2, and sensitivity by a factor of almost 4, compared with the conventional Anger camera (3). The Discovery NM530c enables the acquisition of images not only in the supine position but also in the prone position. Images were reconstructed on a dedicated workstation (Xeleris, GE Healthcare) with an iterative algorithm using the maximum a posteriori expectation maximization method. In addition, a shorter acquisition-time image can be reconstructed using list-

mode.

Comparison of the Discovery NM530c with the standard Anger camera

We prospectively compared the diagnostic performance of the Discovery NM530c with a standard 3-head gamma camera in 150 consecutive patients who underwent a 1-day stress-rest ^{99m}Tc -sestamibi or ^{99m}Tc -tetrofosmin imaging protocol. The radioisotope dosages were 296-370 MBq for stress imaging and 740 MBq for rest imaging. The image acquisition times were 5 and 3 minutes (stress and rest, respectively) using the Discovery NM530c compared with 15 minutes for each

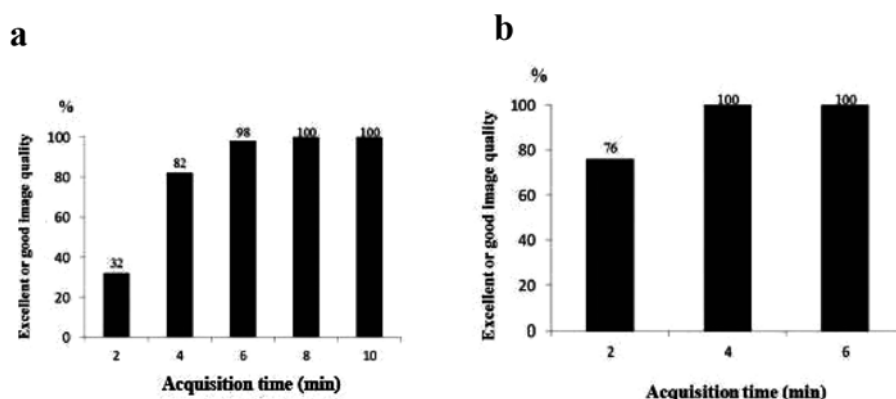


Fig. 2 Prevalence of excellent/good ratings of SPECT image according to scan time in stress imaging (a) and rest imaging (b) with low-dose scan. Reproduced with permission from Hida et al (9).

when using a standard 3-head gamma camera. The summed stress score (SSS), summed rest score (SRS), and summed difference score (SDS) were compared using linear regression analysis (Fig. 1). Strongly positive correlations of 0.83-0.95 were observed. The Bland-Altman limits of agreement for summed scores were -3.8 to 5.7 for SSS, -3.4 to 5.0 for SRS, and -2.7 to 3.0 for SDS (Fig. 1). In 139 patients (93%) who successfully completed left ventricular (LV) functional analysis with electrocardiogram-gated SPECT, linear regression analysis was performed to compare the functional parameters (LV end-diastolic volume, LV end-systolic volume, LV ejection fraction) at rest between the CZT at the 3-minute scan time and the standard Anger camera acquisitions. This analysis produced strongly positive correlations of 0.93-0.98. The Bland-Altman limits of agreement were -16.7 to 9.8 for LV end-diastolic volume, -14.2 to 9.4 for LV end-systolic volume, and -7.7 to 12.1 for LV ejection fraction. Per-segment analysis was judged with the use of a 17-segment model, and a total of 2,550 segments in 150 patients were analyzed using the κ statistic. This showed a strong concordance ($\kappa = 0.815$) for perfusion analysis on a per-segment basis, either acquired with the CZT or standard Anger camera (6). This study has demonstrated an advancement in the Discovery NM530c regarding fast data collection without loss of image quality.

Studies of diagnostic value of combined supine and prone myocardial perfusion imaging

Nishiyama et al (7) examined the diagnostic accuracy of combined myocardial perfusion imaging in the supine and prone positions in 276 patients with suspected or known CAD who underwent single-day ^{99m}Tc -tetrofosmin or ^{99m}Tc -sestamibi stress (296-370 MBq)/rest (740 MBq) CZT SPECT and coronary angiography (CAG). In this study, the scan times in the supine position and prone position were 5 minutes each. Sensitivity, specificity, and accuracy for detecting CAD

($\geq 70\%$ luminal narrowing) were analyzed. When the diagnostic value of CZT SPECT imaging was limited to 76 patients in whom CAG was performed, combined supine and prone imaging had a significantly higher specificity (82% vs 50%; $p < 0.001$) and accuracy (85% vs 76%; $p = 0.035$) without loss of sensitivity (85% vs 87%) than supine imaging alone. On a per-vessel analysis, the sensitivity and specificity of the combined supine and prone imaging were 53% and 81% for left anterior descending artery (LAD) stenosis, 72% and 66% for left circumflex (LCx) stenosis, and 74% and 68% for right coronary artery (RCA) stenosis, respectively.

Goto et al (8) also reported that combined supine and prone imaging improved the diagnostic accuracy for the detection of infero-lateral CAD. In this study, 322 patients underwent both a 1-day adenosine stress (370 MBq)/rest (740 MBq) ^{99m}Tc -tetrofosmin MPI using the Discovery NM530c and CAG within 2 months. The scan time was 5 minutes for supine stress and rest imaging, and 3 minutes for prone stress and rest imaging. The presence of obstructive CAD was defined as $\geq 75\%$ stenosis of the artery. To detect angiographically confirmed infero-lateral CAD, combined supine and prone imaging had a significantly higher specificity (93% vs 72%; $p < 0.0001$) and accuracy (88% vs 74%; $p < 0.0001$) than supine imaging alone. The sensitivity of combined supine and prone imaging was not significantly lower than that of supine imaging (68% vs 82%; $p = 0.10$). In addition, although the prevalence of CAD was the highest (69%) in patients with abnormal findings on both supine and prone imaging, the majority of patients (97%) with normal supine and prone imaging did not have CAD. Furthermore, in patients disparate findings between supine imaging and prone imaging, a significant CAD was observed in 14% and 17% of patients with abnormalities in the supine or prone imaging alone, respectively. These data suggest that combined supine and prone imaging with the Discovery NM530c is useful for reducing the false-positive rate in the infero-posterior or

infero-lateral segment associated with supine imaging, and has diagnostic value for detecting obstructive CAD.

Comparison of myocardial image quality and counts between low-dose and standard dose scans

A CZT camera has the potential to shorten the scan time and reduce a patient's radiation exposure. We prospectively compared the myocardial counts and image quality at a low-dose protocol with those at a standard dose protocol. The study group comprised 100 consecutive patients who underwent 1-day stress/rest ^{99m}Tc -tetrofosmin SPECT. The standard dose (296/740 MBq) protocol was performed in 50 patients with a 5-minute scan time for stress imaging and a 3-minute scan time for at rest imaging. The low-dose (185/370 MBq) protocol was performed in 50 patients with a 10-minute scan time for stress imaging and a 6-minute scan time for at rest imaging. Myocardial image quality score was graded on a 4-point scale (1=poor, 2=adequate, 3=good, 4=excellent) and myocardial counts were assessed in both protocols (6). The myocardial image quality scores with the low-dose scans were similar to those with the standard dose scans (3.8 ± 0.4 vs 3.9 ± 0.3 for stress; 3.8 ± 0.4 vs 3.9 ± 0.3 for rest, respectively). In the post-stress scan at the dose of 185 MBq of ^{99m}Tc -tetrofosmin, the prevalence of excellent/good ratings for the SPECT image increased rapidly. At the 6-minute scan time, the prevalence of an excellent/good image reached 98% (Fig. 2a). In the scan at rest with 370 MBq of ^{99m}Tc -tetrofosmin, the prevalence of an excellent/good image already reached 100% at the 4-minute scan time (Fig. 2b). Myocardial counts were similar between the standard dose scan and the low-dose scan with twice as much as the standard dose scan-time in both stress imaging and rest imaging (9). These results suggest that low-dose scan with a longer scan time obtains higher myocardial counts and reduces a patient's radiation exposure without loss of image quality.

Diagnostic performance of the Discovery NM530c as studied by multicenter registry

To assess the diagnostic performance of the Discovery NM530c for a large number of patients, we formed a working group that was supported by the Japanese Society of Nuclear Medicine from 2012 to 2014, and registered 1,000 patients from 4 institutions. The methods for inducing stress were exercise in 153 patients (15%) and vasodilator pharmacologic stress in 847 patients (85%). ^{99m}Tc -radiotracer was used in 711 patients (71%) and ^{201}Tl in 289 patients (29%). Significant coronary stenosis was defined as $\geq 75\%$ diameter narrowing on visual estimation. In all of the 1,000 patients, 74% sensitivity, 85% specificity, and 81% accuracy for LAD stenosis, 76% sensitivity, 89% specificity, and 85% accuracy for LCx stenosis, and 72% sensitivity, 86% specificity, and

82% accuracy for RCA stenosis were observed. According to the radiotracers, in the 711 patients in whom ^{99m}Tc -radiotracer was used, the respective sensitivities, specificities, and accuracies were 66%, 91%, and 83% for LAD stenosis, 76%, 90%, and 87% for LCx stenosis, and 65%, 91%, and 85% for RCA stenosis. In contrast, in the 289 patients in whom ^{201}Tl was used, the respective sensitivities, specificities, and accuracies were 88%, 63%, and 75% for LAD stenosis, 76%, 86%, and 82% for LCx stenosis, and 82%, 71%, and 75% for RCA stenosis (10). These results suggest that the diagnostic sensitivity for LAD with ^{201}Tl may be superior to that with ^{99m}Tc -radiotracer. Thus, additional studies are necessary to evaluate the effects of different radiotracers on the diagnostic performance of CZT SPECT MPI.

Diagnostic performance of the Discovery NM530c in detecting significant coronary stenosis as assessed using fractional flow reserve

Recently, fractional flow reserve (FFR) has been considered as the gold standard for evaluating the physiological significance of epicardial coronary stenosis (11-13). We retrospectively evaluated the diagnostic value of the CZT gamma camera system using thallium-201 in 95 consecutive patients with suspected or known CAD who had undergone CAG and FFR. Image acquisition was performed in the supine and prone positions after stress for 5 minutes and 3 minutes, respectively, and in the supine position at rest for 10 minutes. Significant coronary stenosis was defined as $\geq 90\%$ diameter narrowing on visual estimation or as a lesion of $< 90\%$ and $\geq 50\%$ stenosis with an FFR of ≤ 0.75 . To detect individual coronary stenosis, for an FFR cut-off of 0.75, the respective sensitivities, specificities, and accuracies were 90% 64%, and 78% for LAD stenosis, 78%, 84%, and 81% for LCx stenosis, and 83%, 47%, and 60% for RCA stenosis. The combination of prone and supine imaging resulted in a higher specificity for RCA disease than supine imaging alone (65% vs 47%), with an improvement in accuracy from 60% to 72%. Using thallium-201 with a short acquisition time, combined with prone and supine imaging, CZT SPECT had a high diagnostic yield in detecting significant coronary stenosis as assessed on FFR (14).

On the other hand, with respect to the diagnostic performance of ^{99m}Tc -radiotracer CZT SPECT, we prospectively evaluated 102 consecutive patients with suspected or known CAD with a low-dose stress/rest protocol (^{99m}Tc -radiotracer 185/370 MBq) using CZT SPECT. Image acquisition was performed in the supine and prone positions after stress for 10 minutes and 6 minutes, respectively, and in the supine position at rest for 6 minutes. Within 3 months, coronary angiography was performed and a significant stenosis was defined as $\geq 90\%$ diameter narrowing on visual

estimation, or as a lesion of <90% and $\geq 50\%$ stenosis with an FFR of ≤ 0.80 . To detect individual coronary stenosis, the respective sensitivities, specificities, and accuracies were 86%, 75%, and 82% for LAD stenosis, 76%, 81%, and 79% for LCx stenosis, and 87%, 92%, and 90% for RCA stenosis. As for limiting to 92 coronary lesions in which FFR was measured, stress SPECT showed 77% sensitivity, 91% specificity, and 84% accuracy, whereas the diagnostic value decreased to 52% sensitivity, 68% specificity, and 58% accuracy based only on visual estimation of $\geq 75\%$ diameter narrowing (15). Even using a low-dose technetium-99m (185/370 MBq) 1-day protocol with an effective dose of ≤ 5 mSv, CZT SPECT demonstrated an acceptable diagnostic yield in detecting a significant coronary stenosis as assessed by FFR.

Diagnostic value of myocardial perfusion reserve on dynamic ^{201}Tl SPECT for predicting left main disease and 3-vessel disease

One of the major limitations of myocardial perfusion imaging is its special relativity in perfusion defect analysis (16,17). High-risk groups such as left main disease and multivessel disease may be missed if one relies only on perfusion analysis (18-20). Although positron emission tomography enables the assessment of quantification of myocardial blood flow and myocardial flow reserve (MFR) to identify patients with balanced 3-vessel disease, the conventional Anger camera has a low feasibility of quantifying MFR on dynamic SPECT in the clinical settings (21-23). Miyagawa et al reported to estimate MFR derived from dynamic $^{99\text{m}}\text{Tc}$ -radiotracer SPECT during pharmacologic stress and rest using the Discovery NM530c. Novel software is currently under development in their institution (22). Shiraishi et al (24) examined whether myocardial perfusion reserve (MPR) derived from ^{201}Tl dynamic SPECT using the Discovery NM530c is useful for predicting left main disease and 3-vessel disease. In this study, 55 consecutive patients underwent adenosine stress ^{201}Tl (111 MBq) SPECT and invasive coronary angiography. For stress MPI, a half-dose of ^{201}Tl (55.5 MBq) is injected. Dynamic SPECT images are acquired for 6 minutes and conventional gated SPECT is performed for 7 minutes. At-rest images are acquired 3 hours later, conventional gated SPECT is performed for 7 minutes, a half-dose of ^{201}Tl (55.5 MBq) is injected, and dynamic SPECT images are acquired for 6 minutes. The MPR index was calculated using the standard 2-compartment kinetic model. On multivariate analysis, it was found that an MPR index ≤ 1.5 yielded the highest diagnostic accuracy (odds ratio: 82.3, $p=0.005$). For predicting left main disease and 3-vessel disease, the sensitivity, specificity, and accuracy were 86%, 78%, and 80% for the MPR index. The quantification of MPR using the

Clinical Performance of the Discovery NM530c

Discovery NM530c may help identify balanced ischemia in patients with left main or 3-vessel disease.

Conclusions

The Discovery NM530c, which is one of the new generations of SPECT cameras equipped with CZT detector technology, has been introduced in Japan about 5 years ago. The Discovery NM530c provides superior image quality, reduced acquisition time, and lower radiotracer dose than the conventional Anger camera and shows an acceptable diagnostic accuracy in detecting a significant coronary stenosis not only on visual estimation of $\geq 75\%$ diameter narrowing but also as assessed by FFR. In the future, further reduction in either the scan time or the tracer dose may be possible, even when using a low-dose technetium-99m protocol. Furthermore, the estimation of MFR using the CZT SPECT system may be possible by the accumulation of clinical research.

Acknowledgments

I gratefully acknowledge the invaluable insights and advice of Professor Akira Yamashina and Professor Taishiro Chikamori in writing this review. I thank my colleagues at Tokyo Medical University and all the members of the semiconductor SPECT study (SSS) group. I also appreciate Dr. Edward Barroga, Associate Professor and Senior Editor of Tokyo Medical University for editing the manuscript.

Sources of funding

None declared.

Conflicts of interest

None declared.

Reprint requests and correspondence:

Satoshi Hida, MD

Department of Cardiology, Tokyo Medical University, 6-7-1 Nishishinjuku, Shinjuku-ku, Tokyo, Japan 160-0023

E-mail: hida-bin@tokyo-med.ac.jp

References

1. Cerqueira MD, Allman KC, Ficaro EP, et al. Recommendations for reducing radiation exposure in myocardial perfusion imaging. *J Nucl Cardiol* 2010; 17: 709-18.
2. Kudo T, Ideguchi R. The effects of medical radiation: A few things nuclear cardiologists must know. *Ann Nucl Cardiol* 2015; 1 (1): 35-42.
3. Herzog BA, Buechel RR, Katz R, et al. Nuclear myocardial perfusion imaging with a cadmium-zinc-telluride detector technique: optimized protocol for scan time reduction. *J Nucl Med* 2010; 51: 46-51.

4. Duvall WL, Croft LB, Godiwala T, et al. Reduced isotope dose with rapid SPECT MPI imaging: initial experience with a CZT SPECT camera. *J Nucl Cardiol* 2010; 17: 1009-14.
5. Songy B, Lussato D, Guernou M, et al. Comparison of myocardial perfusion imaging using thallium-201 between a new cadmium-zinc-telluride cardiac camera and a conventional SPECT camera. *Clin Nucl Med* 2011; 36: 776-80.
6. Tanaka H, Chikamori T, Hida S, et al. Comparison of myocardial perfusion imaging between the new high-speed gamma camera and the standard anger camera. *Circ J* 2013; 77: 1009-17.
7. Nishiyama Y, Miyagawa M, Kawaguchi N, et al. Combined supine and prone myocardial perfusion single-photon emission computed tomography with a cadmium zinc telluride camera for detection of coronary artery disease. *Circ J* 2014; 78: 1169-75.
8. Goto K, Takebayashi H, Kihara Y, et al. Impact of combined supine and prone myocardial perfusion imaging using an ultrafast cardiac gamma camera for detection of inferolateral coronary artery disease. *Int J Cardiol* 2014; 174: 313-7.
9. Hida S, Chikamori T, Tanaka H, et al. Comparison of myocardial image quality and counts between low dose and standard dose scans with a cadmium-zinc-telluride semiconductor camera system. *Nuclear Cardiology* 2015; 17: 6-12. (in Japanese).
10. Chikamori T, Goto K, Hida S, et al. Diagnostic performance of a semiconductor gamma camera system as studied by multicenter registry. *J Cardiol* 2016; in press.
11. Tonino PA, De Bruyne B, Pijls NH, et al. Fractional flow reserve versus angiography for guiding percutaneous coronary intervention. *N Engl J Med* 2009; 360: 213-24.
12. De Bruyne B, Pijls NH, Kalesan B, et al. Fractional flow reserve-guided PCI versus medical therapy in stable coronary disease. *N Engl J Med* 2012; 367: 991-1001.
13. Tonino PA, Fearon WF, De Bruyne B, et al. Angiographic versus functional severity of coronary artery stenoses in the FAME study fractional flow reserve versus angiography in multivessel evaluation. *J Am Coll Cardiol* 2010; 55: 2816-21.
14. Tanaka H, Chikamori T, Tanaka N, et al. Diagnostic performance of a novel cadmium-zinc-telluride gamma camera system assessed using fractional flow reserve. *Circ J* 2014; 78: 2727-34.
15. Chikamori T, Hida S, Tanaka N, et al. Diagnostic performance of a cadmium-zinc-telluride SPECT system with low-dose technetium-99m as assessed by fractional flow reserve. *Circ J* 2016; 80: 1217-24.
16. White CW, Wright CB, Doty DB, et al. Does visual interpretation of the coronary arteriogram predict the physiologic importance of a coronary stenosis? *N Engl J Med* 1984; 310: 819-24.
17. Klocke FJ. Cognition in the era of technology: "seeing the shades of gray". *J Am Coll Cardiol* 1990; 16: 763-9.
18. Nygaard TW, Gibson RS, Ryan JM, et al. Prevalence of high-risk thallium-201 scintigraphic findings in left main coronary artery stenosis: comparison with patients with multiple- and single-vessel coronary artery disease. *Am J Cardiol* 1984; 53: 462-9.
19. Iskandrian AS, Heo J, Lemlek J, et al. Identification of high-risk patients with left main and three-vessel coronary artery disease using stepwise discriminant analysis of clinical, exercise, and tomographic thallium data. *Am Heart J* 1993; 125: 221-5.
20. Tanaka H, Chikamori T, Hida S, et al. Diagnostic value of vasodilator-induced left ventricular dyssynchrony as assessed by phase analysis to detect multivessel coronary artery disease. *Ann Nucl Cardiol* 2015; 1 (1): 6-17.
21. Petretta M, Soricelli A, Storto G, et al. Assessment of coronary flow reserve using single photon emission computed tomography with technetium 99m-labeled tracers. *J Nucl Cardiol* 2008; 15: 456-65.
22. Miyagawa M, Nishiyama Y, Tashiro R, et al. Novel cardiac SPECT technology with semiconductor detectors: Emerging trends and future perspective. *Ann Nucl Cardiol* 2015; 1 (1): 18-26.
23. Ito Y, Katoh C, Noriyasu K, et al. Estimation of myocardial blood flow and myocardial flow reserve by ^{99m}Tc-sestamibi imaging: comparison with the results of [¹⁵O] H₂O PET. *Eur J Nucl Med Mol Imaging* 2003; 30: 281-7.
24. Shiraishi S, Sakamoto F, Tsuda N, et al. Prediction of left main or 3-vessel disease using myocardial perfusion reserve on dynamic thallium-201 single-photon emission computed tomography with a semiconductor gamma camera. *Circ J* 2015; 79: 623-31.